MEASUREMENT OF DEVELOPING TURBULENT FLOWS SUBJECT TO PLANE RATE OF STRAIN IN A ROTATING CURVED DUCT OF VARIABLE CROSS-SECTION

Young Don Choi
Department of Mechanical Engineering, Korea University,
Anamdong, Sungpukku Seoul, 136-701, Korea

Chang Min Oh
Dae Woo Motor Company, Chungchundong 199,
Boopyongku, Inchun, 407-053, Korea

ABSTRACT

Hot-wire measurements are reported on the developing turbulent flows subject to plane rate of strain in a rotating 90 deg bend. The cross-section of the bend varies from 100mm × 50mm rectangular shape at the bend inlet gradually to the 50mm × 100mm shape at the bend outlet with remaining a constant area. Data signals from the rotating test section are transmitted through a slip ring to the personal computer which is located at the outside of the rotating disc. 3-dimensional velocity and 6 Reynolds stress components were calculated from the equations which correlate the fluctuating and mean voltage values measured with rotating a slant type hot-wire probe into 6 orientations. The effects of Coriolis and centrifugal forces on the mean motions and turbulence structures are investigated with respect to rotational speed.

INTRODUCTION

According to the development of computational fluid dynamics on the 3-dimensional turbulent flows, study on the optimal design technique by CFD for the flow passage shape of turbomachineries has taken a growing interest. Essential point for the optimal design of the flow passage shape of turbomachines by CFD is to apply the proper turbulence model which can capture the complex turbulent flow behaviors in the rotating curved duct passage. Recently various second moment turbulence closures have been proposed and applied to the practical engineering problems. However, Since the turbulence closures have only been tested in the ideal flow conditions such as plane channel flows or straight flow pipe flows, in order to apply them to the analysis of turbomachinery flows, in practice, they should be at least verified in the rotating curved duct flows which generated strong cross-stream motions associated with the centrifugal and Coriolis forces.

Turbulent flows subject to plane rate of strain in a rotating curved duct of variable cross-section have several qualities that makes it well suited as a bench mark test flow for the development of new second moment turbulence closures. In practical applications, there arise circumstances in which the cross-section of a duct changes shape without a change of area with a consequent distortion of the mean flow, because in the absence of area change there is no rate of strain in the streamwise direction.

Turbulence in a constant area duct with its cross-section rotated through 90 deg in the streamwise direction has been studied both experimentally and computationally by Tucker and Reynolds (1968), Gence and Mathiew(1980), and Choi and Lumley(1984), DNS has been applied to these flows by Lee and Reynolds (1985). However, developing turbulent flows subject to plane rate of strain in a rotating curved duct with a constant area has not yet been studied experimentally or computationally. In such flows, Coriolis and centrifugal forces associated with the rotation of duct as well as the centrifugal force associated with the curvature of duct may act both through the mean motions and turbulence structures.

VARIATION OF REYNOLDS STRESSES IN A CONDITION OF PLANE RATE OF STRAIN.

Figure 1 show the schematic representation of a rotating curved duct with its cross-section rotated through 90° in the streamwise direction. In the present study, two kinds of flow modes are investigated experimentally for a range of rotational speed. One is the inward flow mode in which the flow is suctioned through the test-section toward the center hole which is located at the rotating hollow shaft. The other

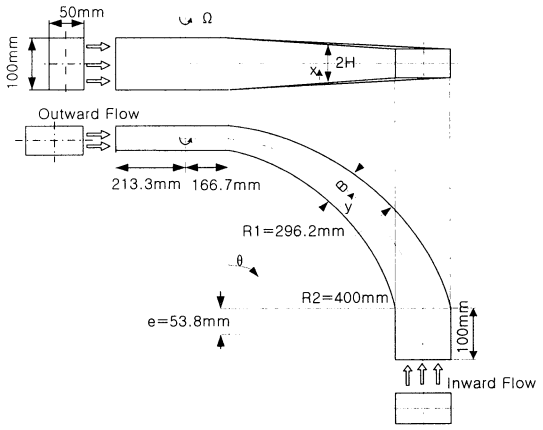

Figure 1. Schematic showing the shape of test section.

is outward flow mode in which the flow is blown out from the hollow shaft toward outward direction. In both cases turbulence is anstrained in the streamwise direction and the rates of strain are confined to the cross-sectional plane. If we confine attention to the neighborhood of the axis of curved duct in the outward flow mode as shown in Figure 1, we take

$$U = \frac{\partial U}{\partial x}x = -Sx \quad \text{and} \quad V = \frac{\partial V}{\partial r}r = \mathrm{S}r \tag{1}$$

where S is a rate-of-strain parameter. If we adopt the linear return to isotropy model and IP(Isotropization of Production) model for the pressure strains, and the isotropic assumption for the dissipation rate of Reynolds stresses yield, the Reynolds stress equations yield

$$\begin{aligned} W\frac{\partial \overline{u^2}}{r\partial\theta} &= -S\left(-2\overline{u^2} + \frac{2}{3}C_2(2\overline{u^2} + \overline{v^2} + \overline{w^2})\right) && ① \\ &\quad -\frac{\varepsilon}{k}\left[C_1(\overline{u^2} - \frac{2}{3}k) + \frac{2}{3}\overline{u^2}\right] && ② \\ &\quad +\frac{2}{3}C_2\overline{vw}\frac{W}{r} && ③ \end{aligned} \tag{2}$$

$$\begin{aligned} W\frac{\partial \overline{v^2}}{r\partial\theta} &= -S\left(2\overline{v^2} - \frac{2}{3}C_2(2\overline{v^2} + \overline{u^2} - \overline{w^2})\right) && ① \\ &\quad -\frac{\varepsilon}{k}\left[C_1(\overline{v^2} - \frac{2}{3}k) + \frac{2}{3}\overline{v^2}\right] && ② \\ &\quad -\frac{4}{3}C_2\overline{vw}\frac{W}{r} && ③ \\ &\quad -4\Omega\overline{vw} && ④ \end{aligned} \tag{3}$$

$$\begin{aligned} W\frac{\partial \overline{w^2}}{r\partial\theta} &= -S\left(2\overline{w^2} - \frac{2}{3}C_2(2\overline{w^2} + \overline{u^2} - \overline{v^2})\right) && ① \\ &\quad -\frac{\varepsilon}{k}\left[C_1(\overline{w^2} - \frac{2}{3}k) + \frac{2}{3}\overline{w^2}\right] && ② \\ &\quad +\frac{2}{3}C_2\overline{vw}\frac{W}{r} && ③ \\ &\quad +4\Omega\overline{vw} && ④ \end{aligned} \tag{4}$$

where $\overline{u^2}$, $\overline{v^2}$, $\overline{w^2}$ are the normal, radial and streamwise Reynolds stresses respectively.

Above equations show that the longitudinal variation of Reynolds stresses in a rotating curved duct with constant area is affected by the plane rate of strain ①, the slow term of pressure strain ②, the curvature of duct ③, and the Coriolis force ④. If we assume that isotropic turbulence flows in the curved duct, the production rate of Reynolds stresses by the plane rate of strain would be

$$\overline{u^2} : S(-2\overline{u^2} + \frac{8}{3}C_2\overline{u^2}) = -0.4\overline{u^2}S \quad < 0 \tag{5}$$

$$\overline{v^2} : S(2\overline{v^2} - \frac{4}{3}C_2\overline{u^2}) = 1.6\overline{u^2}S \quad > 0 \tag{6}$$

$$\overline{w^2} : S(2\overline{w^2} - \frac{4}{3}C_2\overline{u^2}) = 1.6\overline{u^2}S \quad > 0 \tag{7}$$

In the inward flow mode, the signs of the production rates by the plane rate of strain become opposite. Therefore, if the mean velocity and Reynolds stress components are measured in the rotating curved duct flows subject to plane rates of strain, they will be used very importantly as the bench mark test flow data to verify the applicability of new turbulence closures to the analysis of complex turbulent flow fields.

EXPERIMENTAL SYSTEM

A schematic of experimental apparatus of the rotating curved duct is shown in Figure 2. It is composed of a test section of 90 deg bend in which the cross-section changes shape without a change of area, rotating disc of 1.95m diameter, Ag-Ni precision slip ring constructed for the transmission of data signals from the rotating test section to the stationary anemometer, electric power supply for automatic traversing mechanism, variable speed motor,

speed reduction gear mechanism, centrifugal blower, orifice flowmeter and hot-wire anemometer system. Figure 3 shows the upper view of the rotating disc. The lengths of inlet and outlet tangents of the curved duct are 1 and 2.225 hydraulic diameters respectively. The test section is constructed from 8mm thickness perspective sheet providing rigid transparent walls. Honey comb and wire mesh are installed in front of the test section to eliminate the cross-stream motions and turbulences involved in the intake flow. Just after the wire mesh, turbulence generator which is made of 4 mm diameter tube bank in 10 mm pitch is installed to generate uniform intake turbulence. The speed of the rotating disc is controlled by a variable speed motor and a bevel gear speed reduction mechanism. The hot-wire probe is traversed by an automatic mechanism which is installed on the rotating disc. Translation and rotation tolerances of the automatic traversing mechanism are 1/200mm and 1/2 deg respectively. Air flow through the test section is provided by a centrifugal blower and the flowrate is measured by a $D-1/2D$ orifice flowmeter controlled by a gate valve and a bypass system. Measurements were carried out for a Reynolds number of 10,000 based on the bulk averaged velocity W_B, the hydraulic diameter D_H at the bend inlet and fluid kinematic viscosity ν. The rotational speeds of the test section is 0, 30, 45 rpm.

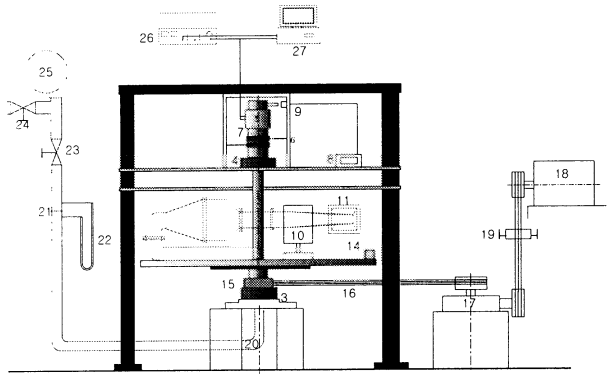

Figure 2. Schematic of the experimental apparatus of the rotating curved duct flow.

1 : Rotating shaft
2 : Rotating disc
3 : Lower bearing
4 : Upper bearing
5 : Slip-ring for hot-wire anemo meter, traversin mechanism
6 : Brush for AC power
7 : Slip-ring for AC power
8 : Tachometer
9 : Contact sensor
10 : Traversing mechanism
11 : Test section
12 : Power supply
13 : Step motor and scanning box driver
14 : Counter balance
15 : V-belt pulley
16 : V-belt
17 : Speed reducer
18 : Variable motor
19 : Roller for V-belt
20 : Stationary pipe
21 : Oriffice
22 : U-manometer
23 : Flow rate control valve
24 : By-pass valve
25 : Blower
26 : Hot-wire anemometer
27 : AD converter
28 : Personal computer

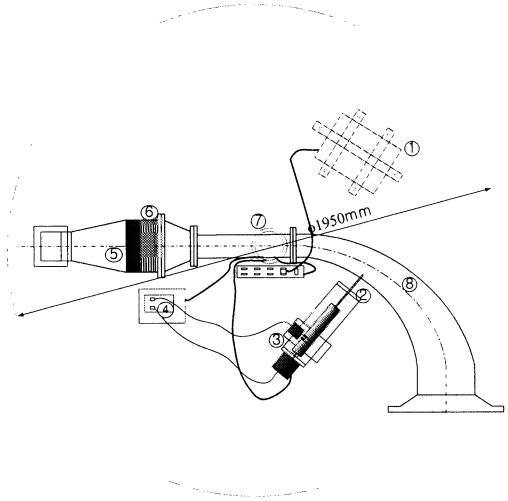

Figure 3. Upper view of the rotating disc.

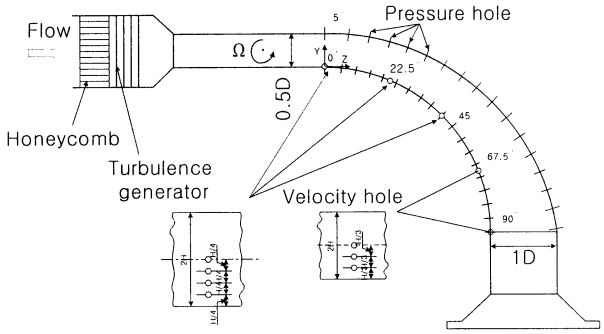

Figure 4. Location of the velocity and pressure holes.

RESULTS AND DISCUSSIONS

Measured pressure coefficients of the inner and outer walls along the symmetry plane of the curved duct are compared in Figure 5 with variation of rotational speed for the inward flow mode. The pressure coefficient is defined as

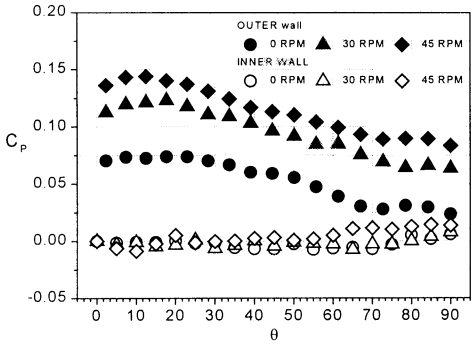

Figure 5. Naviation of pressure coefficients with respect to rotating speed for the inward flow.

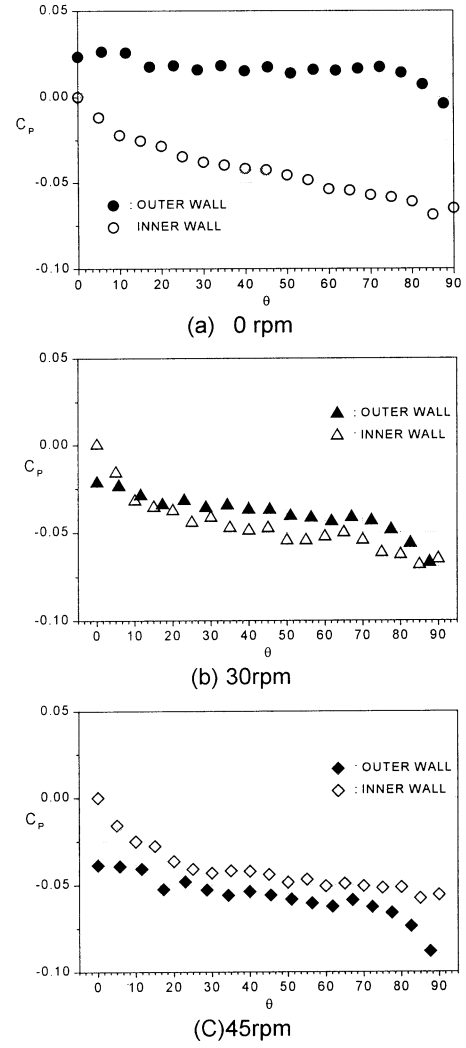

Figure 6. Variation of pressure coefficients with respect to the rotational speed for the outward flow.

$$C_p = \frac{P - P_r}{\frac{1}{2}\rho W_B^2} \tag{7}$$

where W_B is bulk mean velocity , P is local pressure and P_r is reference pressure. Inner wall pressure at the bend inlet was adopted for the reference pressure P_r . As the flow approaches to the stationary curved duct, the pressure coefficients of outer wall rise quickly while those of inner wall drop almost as quickly. However, after short distance into the curved duct, the pressure coefficients of outer wall drop slowly while those of inner wall remain constant. Rotation of the curved duct increases the pressure coefficients of outer wall, but those of inner wall does not change. In the inward flow mode, the radial component of Coriolis force added to the curvature induced centrifugal force in a productive way so that it may increase the difference of pressure coefficients between inner and outer walls. In contrast, in the outward flow mode, the radial component of Coriolis force added to the centrifugal force in a destructive way so that the pressure coefficients of outer wall decrease with the increase of rotational speed. At the rotational speed of 45rpm, the pressure coefficients of outer wall fall below those of inner wall.

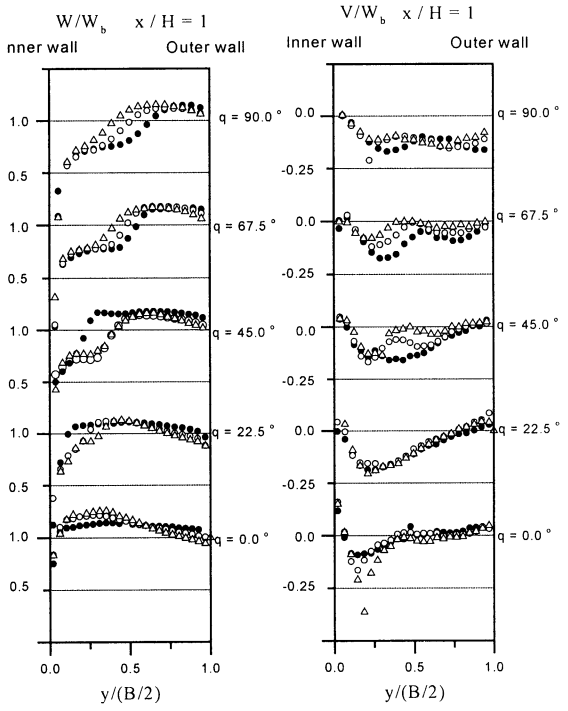

Figure 7. Longitudinal variation of normalized mean streamwise velocity (W/WB) and mean radial velocity (V/WB) along the center symmetry plane.

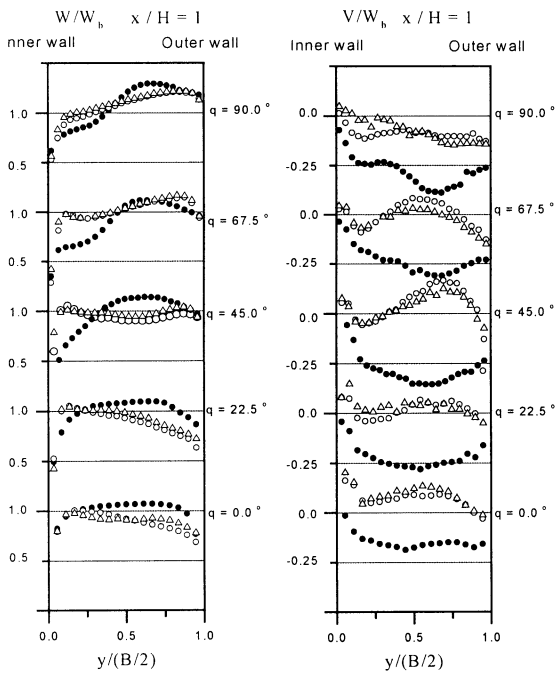

Figure 8. Longitudinal variation of normalized mean streamwise velocity components (W/WB) and mean radial velocity (V/WB) along the center symmetry plane.

Comparison of the variation of streamwise and radial velocity distributions along the symmetry plane of the curved duct for the inward flow mode are shown in Figure 7. As the flow enters the curved duct from the straight inlet tangent, it meets with the abrupt favorable pressure gradient in the inner wall region while the adverse pressure gradient in the outer wall region. A local acceleration and deceleration of the streamwise velocities of inner wall and outer wall sides of the entrance region is partly due to this abrupt pressure gradients in the inner and outer wall regions. Rotation of the curved duct amplifies this local acceleration and deceleration of streamwise velocities in the entrance region. As the flow progresses along the curved duct, the position of maximum streamwise velocities shifts toward the outer wall both in the stationary and rotating flows. However, we can find that the position of the maximum shifts more quickly in the rotating curved duct flow than in the stationary flow. But it stops the moving after θ =45 deg in the rotating curved duct flow while it shift more toward the outer wall in the stationary duct flow. Götler or Dean type vortices engendered in the outer wall region of the rotating curved duct flow may impede the further shifting of the maximum to the outer wall region.

Figure 8 compares the variation of streamwise and radial velocity distributions along the symmetry plane for the outward flow mode between rotating and stationary curved duct flows. In comparison with non-rotating curved duct flow, the profiles of streamwise velocities become so flat. The rather flatter measured profiles may be due to the reduction of secondary flow intensity by the canceling of curvature induced centrifugal force with the radial component of Coriolis force.

In Figure 7 and Figure 8, radial velocity distributions of rotating curved duct flow are shown to be more curved than those of stationary duct flow. Coriolis and centrifugal forces induced by the rotation of the curved duct may promote the break down of counter-rotating vortex pair into multi-cell pattern and it may promote the radial velocity profiles to be more curved.

Secondary flow intensity normalized by streamwise mean velocity at the inlet section are shown in Figure 9 and Figure 10 for the inward and outward flow modes respectively. In the inward flow mode, rotation of curved duct increases the secondary flow intensity up to the plane of 30 deg into the curved duct. But after that station, owing to the break down of counter-rotating vortex pair into multi-cell pattern, the secondary flow intensity does not increase further.

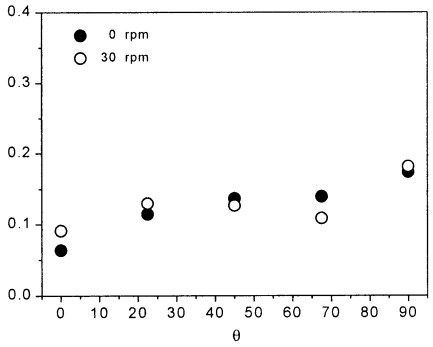

Figure 9. Secondary flow intensity normalized by the bulk mean velocity the inward flow.

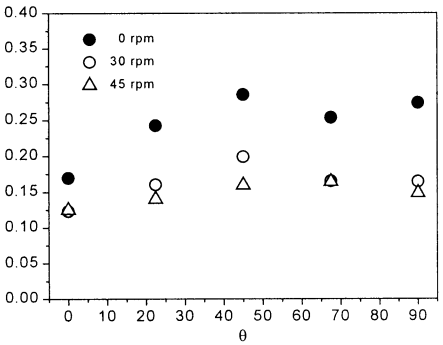

Figure 10. Secondary flow intensity normalized by the bulk mean velocity for the outward flow.

In contrast, in the outward flow mode, the secondary flow intensity was reduced with the increase of rotational speed of curved duct due to the productive adding of Coriolis force to the curvature induced centrifugal forces.

Figure 11 and Figure12 show the longitudinal variation of cross-sectional mean normal stress intensities for the inward and outward flow modes respectively. We can find that the intake turbulence is not isotropic but strongly anisotropic. In this strongly anisotropic intake turbulence condition, we can not find the obvious effect of plane rate of strain in the entrance region of the curved duct, because the longitudinal variation of normal stress intensities in the entrance region are primarily affected by the slow term of pressure strain. However as the flow progresses along the curved duct, the effect of plane rate of strain on the turbulence structures surpasses the effect of slow term of pressure strain. Speed up of the tendency of return to isotropy after the plane of $\theta =$ 65 deg in the inward flow mode while the slow down of it in the outward mode may be caused by this surpassing effect of plane rate of strain over that of slow term of pressure strain on the turbulence structures.

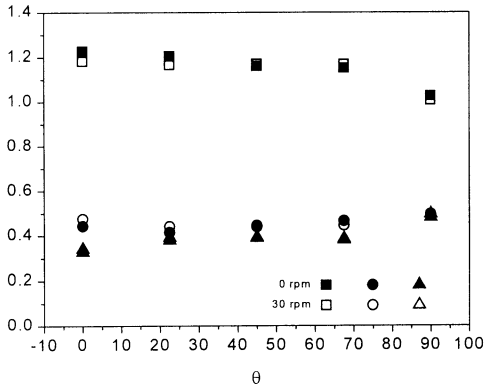

Figure 11 Variation of cross-sectional averaged normal stress intensities for the inward flow

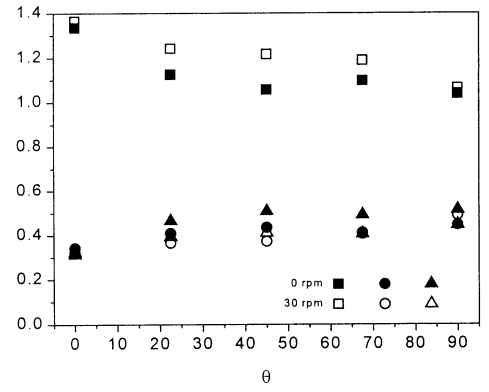

Figure 12 Variation of cross-sectional averaged normal stress intensities for the outward flow

CONCLUSIONS

Present paper reports the hot-wire measurement on the developing turbulent flows subject to plane rate of strain in a rotating curved duct of variable cross section. The following conclusions are obtained

(1) Productive or destructive adding of the radial components of Coriolis force to the curvature induced centrifugal force changes significantly the difference of pressure coefficients between inner and outer walls in the rotating curved duct flow.

(2) In the inward flow mode, rotation of curved duct make shift the position of maximum streamwise velocity more quickly toward the outer wall region than in the stationary flow.

(3) In the outward flow mode, rotation of curved duct make the streamwise velocity profiles so flat due to the destructive adding of the radial component of Coriolis force to the curvature induced centrifugal force.

(4) Due to the strongly anisotropic intake turbulence condition, the effect of plane rate of strain on the turbulence structure only appears in the latter half of the curved duct.

ACKNOWLEDGEMENTS

The work reported here was supported by the project, KOSEP 961-1005-044-2.

REFERENCES

Choi, K.S., and Lumley, J.L. 1984, Return to Isotropy of Homogeneous Turbulence Revisited. In T. Tatsumi(ed.), Turbulence and Chaotic Phenomena in Fluids, Proc. Int. Symp., Kyoto, Japan, 5-10 , September 1983, p. 267.

Gence, J. N., and Mathieu, J., 1980, "The Return to Isotopy of a Homogeneous Turbulence Having Been Submitted to Two Successive Plane Strains," J. Fluid Mech., Vol.15 , p. 201.

Lee, M. J., and Reynolds, W. C., 1985, Numerical Experiments on the Structure of Homogeneous Turbulence, Department of Mechamical Engineering Report TF-24, Stanford University, Stanford, CA.

Libby, P. A., 1996, Introduction to Turbulence, Taylor and Francis, pp. 155-160.

Tucker, H .T., and Reynolds, A. J., 1968, "The Distortion of Turbulence by Irrotational Plane Strain," J .Fluid Mech., Vol.32, p. 657.